This is the submitted version of an article published in Physical chemistry chemical physics. Link to the version of record: http://dx.doi.org/10.1039/C5CP06207A

Mesogen vs. crosslinker resolved molecular order and reorientational exchange using deuteron NMR

Received 00th January 20xx,
Accepted 00th January 20xx

DOI: 10.1039/x0xx00000x

www.rsc.org/

J. Milavec[a,b], V. Domenici[c], B. Zupančič[a], A. Rešetič[a,b], A. Bubnov[d], B. Zalar[a,b]

Differences in the temperature behaviour of orientational ordering of structurally equivalent side-chain liquid single crystal elastomers (LSCEs), ^{2}H-labelled in the crosslinker and mesogen, have been studied by deuteron quadrupole-perturbed NMR. The impact of nematic director reorientations on the deuteron NMR spectral shapes was analyzed in terms of discrete reorientational exchange model. This provided for the determination of the degree of domain or nematic director alignment and for the quantification of the influence of the reorientational exchange on the ^{2}H NMR spectra in terms of two parameters, the nematic director orientational dispersion parameter σ_θ and the motional effectiveness parameter α, respectively. Comparative analysis of model simulations and experimental spectra reveals that mesogenic molecules in oriented LCEs exhibit faster reorientational dynamics as compared to crosslinker molecules and that mesogens and crosslinkers exhibit similar and rather substantial static director orientational disorder.

Introduction

Liquid crystal elastomers (LCEs) are materials in which orientational order of conventional liquid crystals is combined with the elasticity of polymer networks[1–3]. Many interesting properties are expected to emanate from the coupling between nematic liquid crystalline order and elastic deformation, among them the giant thermomechanical response[4]. One of the most exciting features of these materials is their macroscopic form changes as a result of the order-disorder transition of the mesogen. A desired unidirectional alignment of domains in the sample can be achieved by mechanical stretching during the preparation,[5] leading to the so called liquid single crystal elastomers (LSCEs). LCEs are shape-memory materials, due to the ability to memorize the macroscopic shape under specific conditions[6]. With increasing temperature, monodomain LSCEs exhibit a mechanical deformation, specifically a thermomechanical contraction, related to disordering and thermal motion of mesogenic molecules, attached to the polymer backbone[1,7]. They are very good candidates for different technological applications, such as artificial muscles, smart surfaces, microelectromechanical systems (MEMS), and nanoelectromechanical systems (NEMS)[8–11].

^{2}H NMR spectroscopy revealed to be very useful to investigate local molecular orientational behavior of these interesting materials[4,12–15]. LSCEs are multicomponent systems, consisting of a polymer backbone and one or several different types of crosslinking moieties and mesogens. It is anticipated that individual components exhibit different orientational ordering and segmental dynamics. In previous researches[4,12,15], this aspect of LSCE systems has never been addressed in a greater detail. Specifically, no comparative studies targeted towards elucidating possible differences in the ordering of crosslinker vs. the ordering and dynamical behavior of mesogen have been performed so far. For this reason, we are reporting a systematic study on a series of conventional and newly synthesized siloxane-based side-chain liquid single crystals elastomers (LSCEs) by developing a new, component-resolved NMR methodology.

The molecular dynamics influences the NMR spectra. Typical molecular motions are: (i) high-frequency reorientations of the molecule about its long axis and rotational diffusion of the long molecular axis; (ii) reorientations of the nematic director, equivalently time-averaged direction of the long molecular axis, with an intermediate timescale; (iii) reorientations mediated by translational displacements (RMTD) mechanism[16] with a rather long timescale set by molecular translational diffusion in an environment with spatially inhomogeneous nematic director[17,18]. In general, three characteristic motional narrowing regimes exist, depending on the timescale of molecular dynamical processes, that impact the relation between deuteron quadrupole-perturbed NMR frequency and molecular orientational or conformational state. The particular motional averaging regime is determined by the ratio between the "rigid lattice" spectral line width (corresponding to the inhomogeneously broadened spectrum of a ^{2}H-labelled molecule with many orientational and conformational states)

[a] *Department of Condensed Matter Physics, J. Stefan Institute, Jamova 39, SI-1000 Ljubljana, Slovenia*
[b] *Jožef Stefan International Postgraduate School, SI-1000 Ljubljana, Slovenia*
[c] *Dipartimento di Chimica e Chimica Industriale, Universitá degli studi di Pisa, via Moruzzi 3, 56124 Pisa, Italy*
[d] *Institute of Physics, Academy of Sciences of the Czech Republic, Na Slovance 2, 182 21 Prague 8, Czech Republic*

and the characteristic frequency, i.e. the inverse timescale, of the dynamic process providing for reorientational exchange among these instantaneous states.

In the "fast motion regime", when the motion's characteristic correlation time is short, typically τ_c <10^{-7} s, motional narrowing sets in and the inhomogeneous spectrum is completely averaged-out into a homogeneously broadened spectral line with a Lorentzian line shape. Its line width (fwhm) is related to the spin-spin, equivalently transversal, relaxation time T_2 via[17]

$$fwhm_{hom} = \frac{1}{\pi T_2}. \quad (1)$$

This is a situation encountered with liquid crystals at high temperatures, in the isotropic state, where a single line is found at the Larmor frequency, since S=0. With decreasing temperature, reorientational motions are slowed-down, τ_c increases and, consequently, T_2 becomes shorter, resulting in increasing $fwhm_{hom}$ with decreasing temperature. For even slower molecular motion, with the characteristic correlation time in the intermediate range (typically 10^{-7} s ≤ τ_c ≤ 10^{-3} s), motional narrowing becomes incomplete, the spectral lines become non-Lorentzian, and the transversal relaxation becomes non-exponential. The total line width and $fwhm_{hom}$ do not match anymore since in this intermediate regime, the spectral lines are only partially averaged out. In the slow motion regime ($\tau_c \geq 10^{-3}$ s), the molecular motions are too slow to affect the NMR line shape and there are no motional averaging effects. This is why at low temperatures, e.g. in the crystal phase of a liquid crystal elastomer, the spectrum is inhomogeneously broadened and reflects the distribution of instantaneous molecular orientational and conformational states, i.e. the "rigid lattice" state of the system[18,19]. Specifically, if this distribution is isotropic, a Pake-pattern spectral shape is obtained in the rigid lattice limit[20].

The impact of various molecular dynamics processes is best estimated by considering the shift of the ^{2}H quadrupole-perturbed NMR absorption line doublet ($\pm$ sign) as a function of parameters S, β, and θ:

$$\nu^{\pm} = \pm\frac{3}{4}\nu_Q S P_2(cos\beta) P_2(cos\theta) = \pm\frac{3}{4}\bar{\nu}_Q S P_2(cos\theta) \quad (2)$$

Here ν_Q is the quadrupole frequency of the deuteron in a C-D bond, typically 180 kHz[21], the P_2 terms are the respective second Legendre Polynomials of the angle θ between the director of the nematic phase and the magnetic field, and of the angle β between the C-D bond and the molecular main axis. Specifically, $\beta \approx 60°$ for the planar hexagonal geometry of the C-D bond in the case of phenyl ring deuteration. The respective effective quadrupole frequency is $\overline{\nu_Q} \approx 22$ kHz. S is the nematic order parameter.

Both $\bar{\nu}_Q$ and S are averages, the former over fluctuating values of β (for the case of phenyl ring deuteration) and the latter over reorientational fluctuations of the long molecular axis. The inverse characteristic times of these two processes are much shorter than the width of inhomogeneous frequency distribution $\delta\nu \approx 3/4 \cdot \nu_Q \approx 3/4 \cdot 180$ kHz scanned by the reorienting and conforming molecule in the course of time. It is thus plausible to assume that, with respect to both processes, ^{2}H quadrupole-perturbed NMR probes the system in the complete motional narrowing limit. Nevertheless, below the nematic-isotropic transition temperature, although still fast enough for strong motional narrowing, molecular reorientations are biased (non isotropic), a situation described by $S \neq 0$ that leads to onset of doublet splitting (Eq. (2)).

Dynamical processes may also exist in LSCEs, which modulate S and $P_2(cos\theta)$ on much longer timescales, e.g. the RMTD process. In a network with statically misaligned domains and no interdomain mesogen exchange, the spectrum exhibits inhomogeneous broadening, reflecting the distribution of directors through the $P_2(cos\theta)$ term of Eq. (2). However, in the case when either (i) the mesogen molecule performs translational diffusion across domains with misaligned directors, or (ii) the domain director fluctuates in time, partial or complete motional averaging of the spectrum is observed.

Experimental

Materials and methods

^{2}H quadrupole-perturbed NMR spectroscopy. ^{2}H NMR experiments were carried out with a Bruker Advance III 500 MHz high-resolution solid-state NMR spectrometer, equipped with an 11.74 T Bruker Ultrashield superconducting magnet, at a Larmor frequency of 76.753 MHz for deuteron. Spectra were recorded as a function of temperature by applying the quadrupolar echo sequence (90x - τ - 90y- τ - ACQ) with a 90° pulse of 3.8 μs. The echo delay τ was fixed to 10 μs and the delay between consecutive acquisitions was 28 ms. Measurements were performed on a strip-like sample of about 4 mm × 8,5 mm area. In our geometry, the long edge of the sample, the nematic director (oriented along the long edge), and spectrometer field were all pointing vertically. Temperature was controlled to within 0.1 K accuracy. Thermal equilibration of the sample took about 1000 s at each temperature. Lorentzian line fitting was employed to quantitatively determine the line widths of the spectral lines.

Transverse relaxation time T_2 was measured by applying 2D pulse programme with solid-echo sequence (90° - τ - 90° - τ - ACQ) and EXORCYCLE[22] phase cycling, in the temperature range between 370K and 300K. The variable time delay τ ranged from 10 μs to 20 ms (10 values) and 1024 - 20480 scans have been acquired for each spectrum. T_2 values were determined by fitting the experimental integrals of the quadrupole-perturbed ^{2}H spectrum as a function of τ by using exponential decay function.

Preparation of Liquid Single Crystal Elastomers. Several monodomain LSCE samples were made by thermal polymerization followed by the two step crosslinking "Finkelmann procedure"[5]. A pre-polymerization mixture was prepared by adding the poly(methylhydrosilane), the crosslinker V1 (15 % mmol units), the mesogen M4 (33,6 % mmol units) and the mesogen M11 (51,5% mmol units) (see Scheme 1) to a 2.2 ml of anhydrous toluene. 30 μl of commercial platinum catalyst (COD from Wacker Chemie) was added to the final mixture. In a single sample, only one of the

components was used in a deuterated version, which allowed for selective ^{2}H NMR measurements. Preparation of V1, M4, M11 and their deuterated homologues is reported elsewhere[23,24]. The prepared mixture was inserted in a circular reactor inside a temperature-controllable centrifuge. A rate of 5500 rpm (revolutions per minute) and a temperature of 343 K were set for 1 h in order to obtain, in the first step, a partially crosslinked elastomeric network in the form of a film (dimensions 15 mm x 215 mm and thickness of about 0.3 mm). The second crosslinking step consisted of a slow removal of the solvent, accompanied by continual increase of mechanical load (by adding weights) at room temperature. Finally, the sample was dried for 3 days at 343 K and at constant mechanical load.

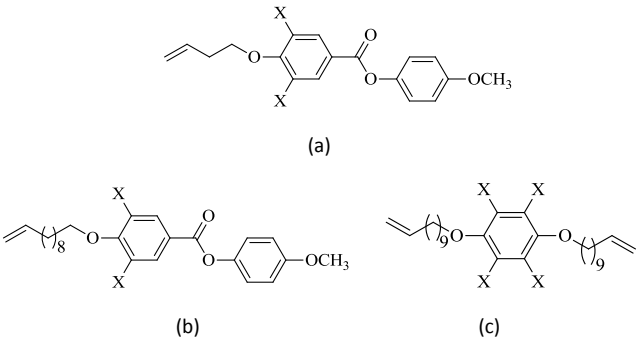

Scheme 1. Moieties used to prepare the LSCEs: (a) mesogen M4, (b) mesogen M11 and (c) crosslinker V1. X=^{2}H in deuterated compounds.

Results and discussion

Director reorientation mechanism and domain misalignment. To estimate which motion regime should be assigned to our spectra of monodomain LSCE ^{2}H-labelled on mesogen or crosslinker molecules, the homogeneous line width and total line width of spectral lines are compared (Fig. 1). In LSCEs with ^{2}H-labelled mesogen, the matching between the homogeneous line width $fwhm_{hom}$ in the nematic phase and the total line width of the spectral line is higher if compared with ^{2}H crosslinker-labelled LSCEs. This suggests that, assuming imperfect domain alignment, director reorientations are mechanism is more effective in the case of mesogen molecules than in the case of crosslinker molecules, confirming the scenario of less restricted reorientational dynamics for the case of mesogen.

In the paranematic phase, one can observe an almost complete matching between homogeneous and total line width for ^{2}H mesogen-labelled LSCEs. Higher temperature results in a faster translation diffusion and therefore the averaging is more effective, while the variations of order parameter are small.

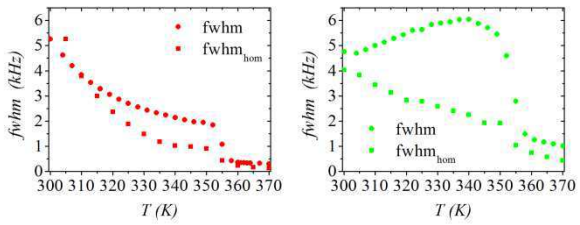

Figure 1. Comparison of homogenous line width (as calculated from the T_2 measurements) and total linewidth for LSCEs ^{2}H-labelled on (a) mesogen and (b) crosslinker.

In the following, we will analyse the impact of the director reorientation process on the shape of ^{2}H NMR spectra in the framework of a discrete reorientational exchange model, in order to obtain more detailed information on the degree of domain alignment, particularly in view of its temperature dependence. We shall demonstrate that domain misalignment and RMTD-like director reorientation in LSCEs can well be quantified by only two parameters, the domain order parameter Q_{stat} and the characteristic order parameter decay time τ_Q.

Theoretical Calculations

Distribution of domain directors. In oriented LSCEs, the distribution of orientations of domain director, $w_{stat}(u,\sigma_\theta)$, is assumed to be spherical Gaussian:

$$w_{\mathrm{stat}}(u,\sigma_\theta)=\frac{e^{-\frac{1-u^2}{\mathrm{tg}^2\sigma_\theta}}}{e^{-\frac{1}{2}\mathrm{ctg}^2\sigma_\theta}\sqrt{2\pi}\,\mathrm{erfi}\left(\frac{\mathrm{ctg}\,\sigma_\theta}{\sqrt{2}}\right)\mathrm{tg}\,\sigma_\theta}. \quad (3)$$

Here $u=\cos\theta\in[-1,1]$, with θ denoting the orientation of a given domain, whereas σ_θ represents the width of the distribution. erfi is the imaginary error function. By introducing $tg\sigma_\theta=\sigma_u$ one can rewrite

$$w_{\mathrm{stat}}(u,\sigma_u)=\frac{e^{-\frac{1-u^2}{2\,\sigma_u{}^2}}}{e^{-\frac{1}{2\,\sigma_u{}^2}}\sqrt{2\pi}\sigma_u\mathrm{erfi}(\frac{1}{\sqrt{2}\sigma_u})}. \quad (4)$$

$w_{\mathrm{stat}}(u)=1/2$ is constant for isotropic distribution of domains, a situation present in polydomain samples. In the above relations we assumed cylindrical symmetry of domain misalignments.

The domain orientational order parameter $Q_{\mathrm{stat}}\equiv\overline{P_2(cos\theta)}$ can be expressed as

$$Q_{\mathrm{stat}}(\sigma_u)=\int_{-1}^{1}w_{\mathrm{stat}}(u,\sigma_u)\frac{(3u^2-1)}{2}\mathrm{d}u=-\frac{1}{2}-\frac{3\sigma_u{}^2}{2}+\frac{3e^{\frac{1}{\sigma_u{}^2}}}{\sqrt{2\pi}\,\mathrm{erfi}\left(\frac{1}{\sqrt{2}}\sigma_u\right)} \quad (5)$$

and the static second moment as

$$M_{2,\mathrm{stat}}(\sigma_u)=\int_{-1}^{1}w_{\mathrm{stat}}(u,\sigma_u)(1-u)^2\,\mathrm{d}u=1-\sigma_u+\frac{e^{\frac{1}{\sigma_u{}^2}}\sqrt{\frac{2}{\pi}}\sigma_u}{\mathrm{erfi}(\frac{1}{\sqrt{2}\sigma_u})}. \quad (6)$$

Transversal precession of magnetization in the case of reorienting nematic director. The Bloch equation for the magnetization *M*, precessing in the plane perpendicular to the

external magnetic field, with nematic director subject to RMTD or RMTD-equivalent director reorientation process, is expressed as[17,19,25]:

$$\frac{\partial M}{\partial t} = i2\pi\nu^{\pm}M - \frac{M}{T_2} + D\nabla^2 M \,, \qquad (7)$$

where the extra term $D\nabla^2 M$ represents the contribution of the diffusion to the rate of change of the magnetization, and T_2 the spin-spin (transverse) relaxation rate of the magnetization.

In the following, we will solve the differential Eq. (7) in a discrete approximation[18]. For arbitrary distribution $w_{\text{stat}}(u,\sigma_\theta)$, we introduce a new "isoprobability" variable $v(u,\sigma_u)$ with respect to which the probability density $w_{stat}(v,\sigma_\theta)$ is constant:

$$v(u,\sigma_u) = \int_{-1}^{u} w(u',\sigma_u)du' = \frac{1}{2}\left(1 + \frac{\text{erfi}\left(\frac{u}{\sqrt{2}\sigma_u}\right)}{\text{erfi}\left(\frac{1}{\sqrt{2}\sigma_u}\right)}\right) . \qquad (8)$$

The isoprobability variable $v \in [0,1]$ is introduced in order to simplify the calculation, specifically to allow for the use of a relatively simple form of discrete exchange matrix K[18], assuming that, in the equilibrium, all the discrete orientational states are equally probable. We discretize the problem by dividing the tilt (θ) coordinate space into *N* equidistant intervals.

The discrete form of Eq. (7) is then obtained by rewriting the derivatives in terms of differences[18].

$$\dot{\boldsymbol{M}}(t) = \left(i\underline{\boldsymbol{\Omega}} - \frac{1}{T_2}\underline{\mathbf{I}} + \frac{1}{\tau}\underline{\mathbf{K}}\right)\cdot\boldsymbol{M}(0) = \underline{\boldsymbol{\mathcal{K}}}\cdot\boldsymbol{M}(0) \,. \qquad (9)$$

$\underline{\boldsymbol{\mathcal{K}}} = \left(i\underline{\boldsymbol{\Omega}} - T_2^{-1}\underline{\mathbf{I}} + \tau^{-1}\underline{\mathbf{K}}\right)$ represents the magnetization exchange matrix in inverse second units (s^{-1}). $\underline{\boldsymbol{\Omega}}$ is the diagonal matrix of magnetization precession frequencies, $\Omega_k = \omega_k^{\pm}$, $\underline{\mathbf{I}}$ the identity matrix, and $\underline{\mathbf{K}}$ the dimensionless population exchange matrix[18].

The nominal exchange time is given by $\tau = 4\Delta v^2/\omega_D$. The initial equilibrium magnetization equals

$$\boldsymbol{M}(0) = (1,1,\cdots,1,1)/N \,. \qquad (10)$$

This is so since the magnetization states are parametrized by the isoprobability variable v and are therefore equally probable in the equilibrium. The formal solution to equation (9) is in terms of matrix exponent of magnetization exchange matrix $\underline{\boldsymbol{\mathcal{K}}}$:

$$\boldsymbol{M}(t) = \exp\left(\underline{\boldsymbol{\mathcal{K}}}t\right)\cdot\boldsymbol{M}(0) \,. \qquad (11)$$

Generalized dimensionless population exchange matrix. In the "weak-collision" limit the exchange only takes place between two neighbouring sites ($\Delta N = 1$), equivalently $\underline{\mathbf{K}}$ is tridiagonal. With the above model, , the "strong-collision" case, the exchange is effective between a general pair of states ($1 \le \Delta N \le N-1$), can as well be addressed, by solely generalizing the exchange matrix to include more distant off-diagonal terms, provided that it satisfies the principle of detailed balance[26]. In our specific case of homogeneous equilibrium (stationary) state (Eq. (10)), this requires that the sum of all elements in any row or column vanishes.

Relaxation dynamics of the orientational order parameter. As discussed above, any dynamic reorientation of nematic director, with characteristic time of the order of or shorter than the inverse rigid lattice line width, should result in the motional narrowing of the spectra. Let us now relate this reorientational process with the exchange modelling presented above. We conjure that at time $t = 0$, the system is ideally ordered, $w(u, t=0) = (\delta(u-1) + \delta(u+1))/2$, and relaxes in the course of time towards the stationary distribution, $w(u, t\to\infty) \to w_{\text{stat}}(u,\sigma_u)$ (relation (4)). Within the discrete exchange model, introduced above, this is equivalent to the initial probability vector

$$\boldsymbol{P}(0) = (1,0,0,\cdots 0,0,1)/N \,, \qquad (12)$$

subject to exchange dynamics

$$\dot{\boldsymbol{P}}(\tilde{t}) = \underline{\mathbf{K}}\cdot\boldsymbol{P}(0) \qquad (13)$$

solving to

$$\boldsymbol{P}(\tilde{t}) = \left(P_1(\tilde{t}), P_2(\tilde{t}), \cdots, P_{N-1}(\tilde{t}), P_N(\tilde{t})\right) = \exp\left(\underline{\mathbf{K}}\,\tilde{t}\right)\cdot\boldsymbol{P}(0) \,. \qquad (14)$$

We have introduced dimensionless time $\tilde{t} = t/\tau$ as the relative time with respect to the nominal exchange time τ. According to solution (14), there exist N characteristic dimensionless times $\tilde{\tau}_j$ of the exchange process, corresponding to negative inverse values of the dimensionless eigenvalues of the population exchange matrix, $\tilde{\tau}_j = -\kappa_j^{-1}$. In a system modelled with a general exchange matrix $\underline{\mathbf{K}}$ and large number of sites N, these times span a broad range from short ones of the order of 1 towards very large values. The stationary state

$$\boldsymbol{P}_{\text{stat}} = \boldsymbol{P}(\tilde{t}\to\infty) = (1,1,\cdots,1,1)/N \qquad (15)$$

is associated with diverging characteristic time, equivalently with $\kappa = 0$ that solves $\dot{\boldsymbol{P}}(\tilde{t}) = \underline{\mathbf{K}}\cdot\boldsymbol{P}_{\text{stat}} = 0$.

It is rather tedious to quantify the reorientational exchange by a spectrum of relaxation times. We simplify the description by regarding this process in terms of the associated decay of the orientational order parameter

$$Q(t) = \int_{-1}^{1} \frac{3u^2-1}{2} w(u,t)du \,, \qquad (16)$$

expressed in the framework of chemical exchange among N nematic director orientational states as

$$Q(\tilde{t}) = \sum_{j=1}^{\tilde{N}} \frac{\tilde{P}_j(\tilde{t})\left(3cos^2 u_j - 1\right)}{2} \qquad (17)$$

Specifically, the evolution of $\boldsymbol{P}(\tilde{t})$ from $\boldsymbol{P}(0)$ to $\boldsymbol{P}_{\text{stat}}$ is associated with the evolution of $Q(\tilde{t})$ from the initial ideal order $Q(\tilde{t}=0) = 1$ towards $Q(\tilde{t}\to\infty) \to Q_{\text{stat}}$. Note that the sum in Eq. (17) is performed over N' discrete sites with probabilities $P_j'(\tilde{t})$ in the space of variable u, whereas the probabilities $P_k(\tilde{t})$ of relation (14) are calculated in N discrete points of isoprobability variable v, typically with numerical methods. In order to calculate $Q(\tilde{t})$ using definition (17), one must transform vector $\boldsymbol{P}(\tilde{t})$ into $\boldsymbol{P}'(\tilde{t})$ by assigning v_k points to equidistant u_j points via the relation $u(v,\sigma_u)$, the latter being the inverse function of $v(u,\sigma_u)$ (Eq. (8)). Δu must be set to a small enough value (equivalently high enough N' must be chosen) so that the calculation accuracy is retained with the above transformation. In particular, for small σ_u of well-aligned samples, this implies $N' \gg N$.

The decay in $Q(\tilde{t})$ is inherently multi-exponential (N different characteristic times within the discrete chemical exchange approximation, see above), and can be expressed as

$$Q(\tilde{t}) - Q_{\text{stat}} = (1 - Q_{\text{stat}})f(\tilde{t}). \qquad (18)$$

The decay function $f(\tilde{t})$ is monotonously decreasing with time from the initial value $f(\tilde{t}=0)=1$ to $f(\tilde{t}\to\infty)=0$.
We now introduce the dimensionless nominal Q-decay time $\tilde{\tau}_Q=\tau_Q/\tau$ as the time during which $f(\tilde{t})$ decreases to 1/2:
$Q(\tilde{\tau}_Q)-Q_{\text{stat}}=(1-Q_{\text{stat}})/2 \Rightarrow \tilde{\tau}_Q(\sigma_u,N,\Delta N)$. (19)

As both $Q(\tilde{t})$ and Q_{stat} depend on σ_u, N, and ΔN, so does $\tilde{\tau}_Q=t_Q/\tau$. A representative $Q(\tilde{t})$ decay is shown in Fig. 2.

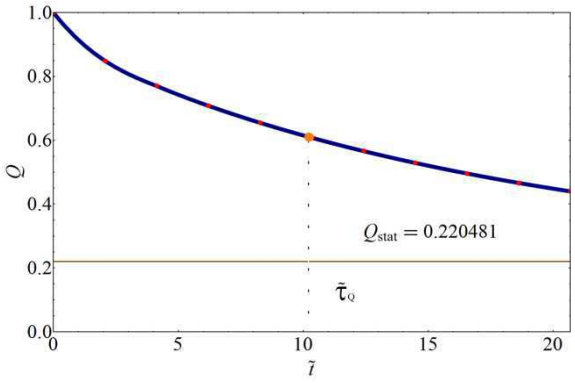

Figure 2. Time dependence of the dynamic orientational order parameter $Q(\tilde{t})$ in a partially-aligned sample with $\sigma_\theta=30°$ ($\sigma_u=0.58$). The point that determines the nominal Q-decay time is marked with the orange dot. Points in red colour were calculated using Eqs. (14) and (17) with $N=100$ and $\Delta N=3$. Blue solid line is an interpolated guide to the eyes.

It is noteworthy that, in the limit of large N and $\Delta N=1$ (weak collision), the reorientational exchange model, introduced above, readily reproduces conventional diffusion with a Gaussian $w(u,\tilde{t})$ propagator profile

$$w_G(u,\tilde{t})=\frac{1}{\sqrt{2\pi\sigma_u^2(\tilde{t})}}\left(e^{-\frac{(u-1)^2}{2\sigma_u^2(\tilde{t})}}+e^{-\frac{(u+1)^2}{2\sigma_u^2(\tilde{t})}}\right), \quad (20)$$

with $\sigma_u^2(\tilde{t})=2\tilde{\omega}_D\tilde{t}=8/N^2\,\tilde{t}$, characteristic for a $1D$ diffusion process. The definition range of the tilt variable is $u\in[-1,1]$, so that the Gaussian approximation is only valid for $\sigma_u^2(\tilde{t})\ll 1$, equivalently $\tilde{t}\ll N^2/8$, since in this case the distribution does not yet extend considerably towards $u=0$ (no overlap of the positive and negative u branches of the distribution (20)). For larger $\tilde{t}$, the profile of $w(u,\tilde{t})$ becomes non-Gaussian and the relation $N^2\sigma_u^2(\tilde{t})/(8\tilde{t})=1$ is not satisfied anymore.
In the case of Gaussian propagator approximation, the dynamic order parameter can be expressed as

$$Q(\tilde{t})\approx 1-3\sqrt{\frac{2}{\pi}}\sigma_u(\tilde{t})+\frac{3\sigma_u{}^2(\tilde{t})}{2}. \quad (21)$$

Evidently, condition $\sigma_u^2(\tilde{t})\ll 1$ that implies Gaussian profile of $w(u,\tilde{t})$ is equivalent to condition $1-Q(\tilde{t})\ll 1$.

Motional narrowing of deuteron NMR spectral lines. Deuteron NMR spectrum is calculated as a Fourier transform

$$\mathcal{J}(\omega)\propto \text{Re}\left\{\int_{-\infty}^{\infty}\mathcal{M}(t)\text{e}^{-\text{i}\omega t}dt\right\} \quad (22)$$

of the time-dependent transversal magnetization $\mathcal{M}(t)=\sum_{k=1}^{N}M_k(t)$. $M_k(t)$ are the components of the magnetization vector $\boldsymbol{M}(t)$. By combining expressions (10) and (11) one obtains

$$\mathcal{M}(t)\propto \boldsymbol{M}^{\text{T}}(0)\cdot\exp\left(\underline{\boldsymbol{\mathcal{K}}}t\right)\cdot\boldsymbol{M}(0) \quad (23)$$

and consequently[17]

$$\mathcal{J}(\nu)\propto \text{Re}\{\boldsymbol{M}^{\text{T}}(0)\left[\frac{1}{\tau}\underline{\mathbf{K}}-\pi\, fwhm_{\text{hom}}\,\underline{\mathbf{I}}\pm i\left(\underline{\boldsymbol{\Omega}}-\omega\underline{\mathbf{I}}\right)\right]^{-1}\boldsymbol{M}(0)\} \quad (24)$$

using $fwhm_{\text{hom}}=(\pi T_2)^{-1}$ and $\omega=2\pi\nu$. We note again that $\pm$ stands for the two components of the deuteron quadrupole perturbed NMR doublet.
We now relate the spectrum to the relaxation dynamics of the order parameter. The nominal exchange time τ, which determines the nematic director reorientational exchange effectiveness, is related to the nominal Q-decay time via

$$\tau(\sigma_u,N,\Delta N)=\frac{\tau_Q}{\tilde{\tau}_Q(\sigma_u,N,\Delta N)}. \quad (25)$$

One can regard τ_Q as the nominal time characterizing the loss of correlations among orientational states of the nematic director, without knowing the details on the reorientational processes. With a specific choice of orientational distribution (parameter σ_u) and exchange topology (matrix $\underline{\mathbf{K}}(N,\Delta N)$), relation (25) provides for scaling of the nominal exchange rate τ^{-1} with respect to σ_u, N, and ΔN to value $\tau(\sigma_u,N,\Delta N)$ that will result in a desirable τ_Q. The dimensionless scaling denominator $\tilde{\tau}_Q(\sigma_u,N,\Delta N)$ is determined by methodology described in previous subsection.
τ_Q, measured against the rigid lattice line width, is found to determine to what extent the detected spectrum will be motionally averaged. To quantify this, we introduce the "motional narrowing effectiveness" parameter

$$\alpha=(\tau_Q\Delta\omega_{\text{r.l.}})^{-1}, \quad (26)$$

with $\Delta\omega_{\text{r.l.}}=2\pi\Delta\nu_{\text{r.l.}}$ where $\Delta\nu_{\text{r.l.}}$ denotes the rigid lattice line width. $\alpha\ll 1$ represents the rigid lattice regime, $\alpha\approx 1$ the intermediate regime, and $\alpha\gg 1$ the strong motional narrowing regime. $\mathcal{J}(\nu)$ can then be rewritten in terms of α as

$$\mathcal{J}(\nu)\propto \text{Re}\{\boldsymbol{M}^{\text{T}}(0)\left[\alpha\tilde{\tau}_Q 2\pi\Delta\nu_{\text{r.l.}}\,\underline{\mathbf{K}}-\pi\, fwhm_{\text{hom}}\underline{\mathbf{I}}\pm i\left(\underline{\boldsymbol{\Omega}}-\omega\underline{\mathbf{I}}\right)\right]^{-1}\boldsymbol{M}(0)\}. \quad (27)$$

According to above relation, if one knows the rigid lattice line width $\Delta\nu_{\text{r.l.}}$ as well as $\tilde{\tau}_Q(\sigma_u,N,\Delta N)$ and $\underline{\mathbf{K}}(N,\Delta N)$, motional narrowing effects can be reproduced by varying a single parameter α in the range $[0,\infty]$. The usefulness of the α-parametrization is in particular supported by the fact that the intermediate motional narrowing regime is reached at $\alpha\approx 1$ universally for any exchange type, i.e. independently from σ_u, N, and ΔN.

Comparison of simulated and experimental deuteron NMR spectra. Network component-resolved orientational order of structurally equivalent LCE films was determined by studying temperature dependences of the ^{2}H NMR spectra across the paranematic–nematic phase transition of monodomain LCEs, ^{2}H-labelled on either mesogen or crosslinker molecule (Fig. 3 (b),(d)). LCEs are inherently multicomponent systems, so that differences in orientational self-organization necessarily occur even between the mesogen and the crosslinker. This is apparently the case in our LCE networks: at the transition from the high-temperature paranematic phase into low-temperature nematic phase, the crosslinker exhibits a

significantly stronger orientational disorder than the mesogen (Fig. 3 (b,d)). We relate the stronger orientational disorder to the fact that molecules of crosslinker are connected by both ends to the polymer chain. Consequently, they are geometrically more confined and exhibit slower overall reorientational dynamics as compared to the mesogen molecules, attached to the backbone at one end only. The result of a slower crosslinker dynamics and therefore less averaging of the spectral lines are broader spectral features and lower spectral resolution when compared to mesogen molecules. Faster director reorientational dynamics could therefore lead to a stronger motional narrowing of mesogen spectral lines compared to crosslinker spectral lines, rendering the spectra of mesogen only seemingly less inhomogeneously broadened. Within this refined scenario, mesogens and crosslinkers might exhibit similar and rather substantial director orientational disorder.

In order to resolve the above ambiguity, a selection of simulated spectra, calculated with reorientational exchange model and the corresponding experimentally determined spectra of monodomain LCEs are compared on Fig 3. Parameter *N* was set to *N=100* and $\Delta N = 3$ in order to obtain a sufficiently high resolution. The simulated spectra were generated by adjusting three parameters: the motional narrowing effectiveness parameter α, the director orientational disorder parameter σ_θ, and the nematic order parameter S. $fwhm_{hom}$ was determined from T_2 relaxation measurements. For deuterated aromatic rings, S is related to the deuteron quadrupole perturbed NMR doublet splitting $\Delta\nu_q$ (evaluated as the difference between two Lorenzian peaks, fitted to the experimental spectra) as follows[15]:

$$\Delta\nu_q = \frac{3}{2}\nu_Q[S(T)\left(cos\beta - \frac{1}{2}sin^2\beta - \frac{\eta}{6}cos^2\beta + \frac{\eta}{6} + \frac{\eta}{3}sin^2\beta\right)] \quad (28)$$

Here $\nu_Q = 185kHz$ and $\eta = 0.004$ are the quadrupolar coupling constant and asymmetry parameter, respectively, and β defines the angle between the CD bond and para axis of deuteron-labelled phenyl ring of crosslinker (fixed to about 60°).

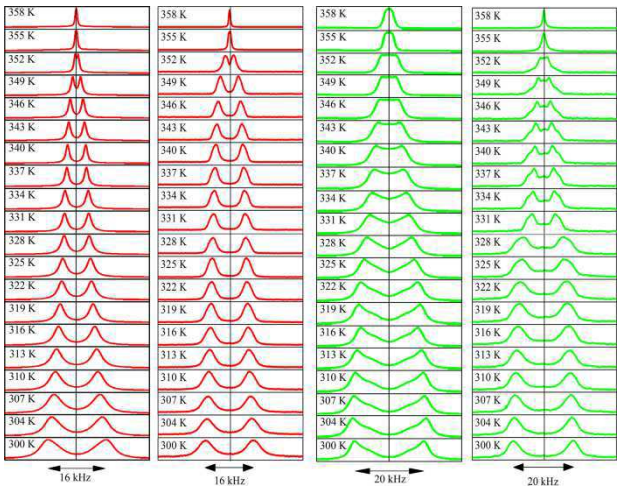

(a) (b) (c) (d)

Figure 3. Series of ^{2}H NMR spectra, calculated from the reorientational exchange model of the nematic director (panel (a, c)) and recorded from the paranematic to the nematic phases on a monodomain LSCE sample with ^{2}H phenyl ring-labelled mesogen M4 (panel (b)) and crosslinker V1 (panel (d)). The respective temperature dependences of the simulation parameters are shown in Fig. 4.

The estimated temperature dependences of the simulation parameters σ_θ and α are presented in Fig. 4 for the two LSCE samples with crosslinker V1 and mesogen M4 deuteration sites, respectively. Similar behaviour of $\sigma_\theta(T)$ is detected in both cases (Fig 4 (a)). At low temperatures, in the temperature interval between 300 K and 320 K, σ_θ monotonously increases and matches within the experimental error for both samples. At temperatures around 330 K a weak anomaly is observed, attributed to the nematic-smectic A transition[27,28]. At temperatures above 350 K, on approaching the paranematic-nematic transition, σ_θ exhibits a substantial increase, particularly in the deuterated mesogen LCE sample. We note that points above 350 K suffer from a large experimental error, both $\sigma_\theta(T)$ and $\alpha(T)$.

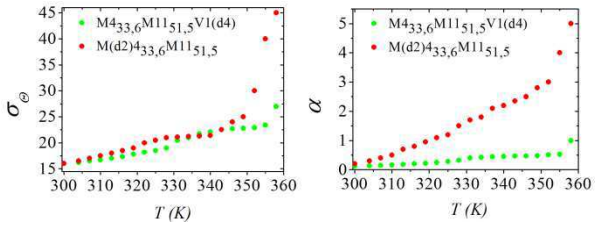

(a) (b)

Figure 4. (a) Domain director alignment parameter σ_θ and (b) motional narrowing effectiveness parameter α as a function of temperature of the two components of the LSCE network: V1 crosslinker molecules (green circles) and M4 mesogen molecules (red circles).

Fig. 4, panel (b) reveals monotonous increase of the motional narrowing effectiveness parameter α with increasing temperature for both types of molecules, demonstrating that reorientational correlation times decrease with temperature and consequently result in a more effective motional narrowing. However, in contrast to $\sigma_\theta(T)$, $\alpha(T)$ is detected to be systematically lower for the crosslinker than for the mesogen, indicative of slower crosslinker's reorientational dynamics. This observation is also compatible with the T_2 magnetization relaxation results (see section Director reorientation mechanism and domain misalignment**)** and thus in further support of scenario in which movement of the crosslinker molecules is more obstructed, since these are attached to the polymer backbone at both ends, compared with the single side only attachment of mesogen molecules.

Conclusions

Differences in the temperature behaviour of orientational ordering of structurally equivalent LCEs, with almost identical mesogen/crosslinker compositions, but different deuteration site, have been studied by ^{2}H NMR. ^{2}H NMR measurements show that crosslinker molecules in LCEs exhibit a significantly

slower overall reorientational dynamics as compared with mesogen molecules, due to their geometrical restrictions originating from stronger attachment to the polymer backbone (both ends for the crosslinker vs. single end for the mesogen). The result of a slower crosslinker dynamics are also broader and more pronounced inhomogeneous spectral features.

The influence of nematic director's orientational disorder and of its reorientational diffusion on the ^{2}H NMR spectra can be described by a simple model of director reorientational exchange, quantified by only two parameters: the static orientational disorder parameter σ_θ and the nominal orientational order decay time τ_Q. Comparative analysis of theoretically modelled and experimentally determined deuteron NMR spectra reveals that both crosslinker and mesogen molecules exhibit similar, substantial static orientational disorder. The disorder is lower at room temperature and monotonously increases on approaching the paranematic nematic transition at about 350 K. The quantitatively similar orientational disorder, detected for the crosslinker and mesogen molecules, is in apparent contradiction with experimentally detected substantially higher inhomogeneous broadening of the crosslinker deuteron spectrum as compared to the mesogen spectrum. Somewhat surprisingly, our results support the scenario of similar degree of orientational disorder, by attributing the mismatch in spectral shapes to faster reorientational dynamics of mesogens, (vs. crosslinker), as identified through much higher value of the motional narrowing effectiveness parameter α.

References

1 M. Warner and E. M. Terentjev, *Liquid Crystal Elastomers*, International Series of Monographs on Physics 120, 2003.
2 W. H. de Jeu, Ed., *Liquid Crystal Elastomers: Materials and Applications*, Springer Berlin Heidelberg, Berlin, Heidelberg, 2012, vol. 250.
3 E. M. Terentjev, *J. Phys. Condens. Matter*, 1999, **11**, R239.
4 V. Domenici, *Prog. Nucl. Magn. Reson. Spectrosc.*, 2012, **63**, 1–32.
5 J. Küpfer and H. Finkelmann, *Makromol. Chem. Rapid Commun.*, 1991, **12**, 717–726.
6 K. A. Burke and P. T. Mather, *J. Mater. Chem.*, 2010, **20**, 3449–3457.
7 V. Domenici, G. Ambrožič, M. Čopič, A. Lebar, I. Drevenšek-Olenik, P. Umek, B. Zalar, B. Zupančič and M. Žigon, *Polymer*, 2009, **50**, 4837–4844.
8 H. Jiang, C. Li and X. Huang, *Nanoscale*, 2013, **5**, 5225–5240.
9 M.-H. Li and P. Keller, *Philos. Trans. R. Soc. Math. Phys. Eng. Sci.*, 2006, **364**, 2763–2777.
10 M. Camacho-Lopez, H. Finkelmann, P. Palffy-Muhoray and M. Shelley, *Nat. Mater.*, 2004, **3**, 307–310.
11 F. Greco, V. Domenici, S. Romiti, T. Assaf, B. Zupančič, J. Milavec, B. Zalar, B. Mazzolai and V. Mattoli, *Mol. Cryst. Liq. Cryst.*, 2013, **572**, 40–49.
12 G. Abbandonato, D. Catalano, V. Domenici and B. Zalar, *Liq. Cryst.*, 2012, **39**, 165–174.
13 V. Domenici, J. Milavec, B. Zupančič, A. Bubnov, V. Hamplova and B. Zalar, *Magn. Reson. Chem.*, 2014, **52**, 649–655.
14 G. Feio, J. L. Figueirinhas, A. R. Tajbakhsh and E. M. Terentjev, *J. Chem. Phys.*, 2009, **131**, 074903.
15 V. Domenici and B. Zalar, *Phase Transit.*, 2010, **83**, 1014–1025.
16 P. J. Sebastião, D. Sousa, A. C. Ribeiro, M. Vilfan, G. Lahajnar, J. Seliger and S. Žumer, *Phys. Rev. E*, 2005, **72**, 061702.
17 A. Abragam, *The principles of nuclear magnetism.*, Clarendon Press, Oxford, 1961.
18 B. Zalar, R. Blinc, S. Zumer, T. Jin and D. Finotello, *Phys. Rev. E Stat. Nonlin. Soft Matter Phys.*, 2002, **65**, 041703.
19 A. Lebar and B. Zalar, *NMR investigation of monodomain liquid crystal elastomer: doctoral thesis*, [A. Lebar], Ljubljana, 2006.
20 B. Cowan, *Nuclear Magnetic Resonance and Relaxation*, Cambridge University Press, Cambridge; New York, 2005.
21 V. Domenici, M. Geppi and C. A. Veracini, *Prog. Nucl. Magn. Reson. Spectrosc.*, 2007, **50**, 1–50.
22 Z. Luz and S. Meiboom, *J. Chem. Phys.*, 1963, **39**, 366–370.
23 V. Domenici, J. Milavec, A. Bubnov, D. Pociecha, B. Zupancic, A. Resetic, V. Hamplova, E. Gorecka and B. Zalar, *RSC Adv.*, 2014.
24 S`achez Ferrer Antoni, *Photo-active liquid crystalline elastomers: doctoral thesis*, Barcelona, vol. 2006.
25 C. P. Slichter, *Principles of Magnetic Resonance*, Springer, Berlin ; New York, 3rd enlarged and updated ed. 1990. Corr. 3rd printing 1996 edition., 1996.
26 M. J. Klein, *Phys. Rev.*, 1955, **97**, 1446–1447.
27 D. M. Lambreva, B. I. Ostrovskii, H. Finkelmann and W. H. de Jeu, *Phys. Rev. Lett.*, 2004, **93**, 185702.
28 W. H. de Jeu, B. I. Ostrovskii, D. Kramer and H. Finkelmann, *Phys. Rev. E Stat. Nonlin. Soft Matter Phys.*, 2011, **83**, 041703.